IOP Conf. Series: Materials Science and Engineering **408** (2018) 012021 doi:10.1088/1757-899X/408/1/012021

An Automatic Aerodynamic Shape Optimisation Framework Based on DAKOTA

C C Xia[1,*], Y J Gou[1], S H Li[1], W F Chen[2] and C Shao[3]

[1] Aerospace System Engineering Shanghai, Shanghai, China
[2] School of Aerodynamics and Astronautics, Zhejiang University, Zhejiang, China
[3] Commercial Aircraft Corporation of China, Ltd. Shanghai, China

*xcc578394953@163.com

Abstract. Aerodynamic design is a must and fundamental aspect for better performance of an aircraft. This work describes a framework for aerodynamic shape optimisation (ASO) based on high-fidelity Computational Fluid Dynamics (CFD) analyses and an open source optimisation toolkit DAKOTA. The free form deformation (FFD) technique is adopted for parameterization of geometries, followed by a transfinite interpolation (TFI) method for grid deformation. CFD simulations are performed by full Navier-Stokes equations in conjunction with turbulence model. CFD, FFD and TFI modules are integrated with DAKOTA by a black-box interface, a pre-processing and a post-processing. The transonic RAE2822 airfoil is employed for demonstration of the effectiveness and capability of the developed framework. Several cases with different optimisation algorithms, design variables and turbulence models are performed. Optimum solutions with significant improvement of lift-drag ratio are presented to demonstrate the capability of the framework in this paper.

1. Introduction

The high fuel-efficiency, long-endurance and emission reduction are the persistent pursuit of modern aircraft. Aerodynamic shape optimisation (ASO) plays an important role in improving the aircrafts' performance and achieving these goals. This can be demonstrated by plenty of particular works, including the design of shock-free airfoil for a commercial airliner [1], the aspiration for better aerodynamic performance of a supersonic rocket [2], and the integration design of afterbody/nozzle with hypersonic cruise vehicle [3]. Extremely abundant researches have been focusing on related techniques in recent decades. Among the various techniques, the Computational Fluid Dynamics (CFD)-based aerodynamic optimisation [4-6] has become an area of intense interest in the past few years, thanks to the development of parallel computing, efficient optimisation algorithms and high-fidelity numerical methods.

With the increasing maturity of CFD and optimisation methods, these two techniques should be more closely connected for further improvement of design efficiency of aircraft, and hence for decreasing of complexity of design process. This may be easily achieved by the help of a robust and automatic optimisation framework. Actually, plenty of past ASO studies have been carried out by several powerful and comprehensive optimisation packages such as Isight, ModelCenter and VisualDOC. Except these commercial toolkits, some open source toolkits are also suitable for scientific and engineering applications, such as the Design Analysis for Optimisation and Terascale

Applications (DAKOTA) [7]. While the open source toolkits are usually not user-friendly, they could be more easily developed for specific problems. Besides, they are more accessible.

In this paper, a CFD-based ASO framework is developed based on the open source optimisation toolkit DAKOTA. In the optimisation flowchart of current study, geometry shapes are parameterized by free form deformation (FFD) method and grid deformation during optimisation is achieved by transfinite interpolation (TFI) method. The aerodynamic characteristics of the airfoil are obtained by solving the Reynolds-averaged Navier-Stokes (RANS) equations. Several optimisation cases are performed for the transonic RAE2822 airfoil and satisfactory results are obtained.

2. Development of the framework

2.1. Parametric modeling

The free form deformation method developed by Sederberg & Parry [8] is used for parameterization in this work. Its original goal was to deform solid surfaces in a free-form manner by moving the control point of the control volume surrounding the object. To be precise, for a given hexahedral control volume, which has a local coordinate system, any point X in it can be described as:

$$\boldsymbol{X} = \boldsymbol{X}_0 + s\boldsymbol{S} + t\boldsymbol{T} + u\boldsymbol{U} \tag{1}$$

where X0 is the origin of control volume and local coordinates s, t and u can be easily solved.

The number of control points will be (l+1)(m+1)(n+1) once the control volume is divided into l, m and n sections in S, T and U directions separately.

Evidently, the global coordinates of the control points can be written as:

$$\boldsymbol{P}_{ijk} = \boldsymbol{X}_0 + \frac{i}{l}\boldsymbol{S} + \frac{j}{m}\boldsymbol{T} + \frac{k}{n}\boldsymbol{U} \tag{2}$$

where i=0,1,…,l, j=0,1,…,m, k=0,1,…,n.

If the control volume is constructed by a trivariate Bernstein polynomial, the global coordinate of an arbitrary point after deformation can be expressed as:

$$\boldsymbol{X}_{new} = \sum_{i=0}^{l}\sum_{j=0}^{m}\sum_{k=0}^{n} B_l^i(s)B_m^j(t)B_n^k(u)\,\boldsymbol{P}_{ijk} \tag{3}$$

where the Bernstein polynomial is defined as:

$$B_l^i(s) = C_l^i(1-s)^{l-i}s^i = \frac{l!}{i!(l-i)!}(1-s)^{l-i}s^i \tag{4}$$

The more detailed operations of FFD can be found in the reference. In this paper, the displacements of the specified control points are regarded as design variables.

2.2. Grid deformation

Once the surface of the geometry changes, the grid should be deformed or regenerated for CFD simulation. Regeneration of the grid might be time-consuming for many cases and deformation is currently the first choice. Since the grid has to be updated at each optimisation step, the robustness and efficiency are of great importance to the method. The transfinite interpolation method used throughout this paper is an algebraic method [9]. A large number of works have shown that satisfactory quality can be maintained by this simple method. The method computes the volume grid points from previously computed displacements of points on the block faces, which are supported by the FFD technique in this work. Taking the RAE2822 airfoil for example, the airfoil shapes, FFD control volumes and meshes before and after deformation are shown in figure 1. Design variables are defined as the displacements in the vertical direction of the six control points between the leading and trailing edges. Both uniformity and orthogonality are maintained after deformation, as can be seen from the figures.

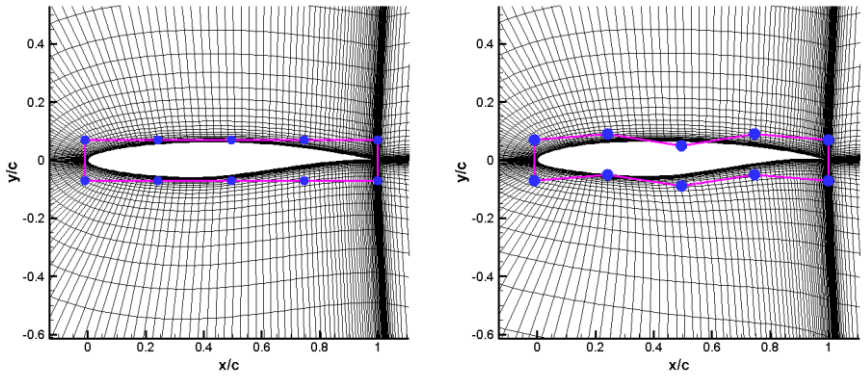

Figure 1. Illustration of the airfoil shape and mesh before (left) and after (right) deformation.

2.3. CFD method

The flow field and aerodynamic coefficients of the airfoil for the current work are obtained by CFD simulation. The three-dimensional full Navier-Stokes equations for steady, compressible flow are selected as the governing equations and can be given as:

$$\frac{\partial \boldsymbol{Q}}{\partial t} + \frac{\partial}{\partial x}(\boldsymbol{E} + \boldsymbol{E_v}) + \frac{\partial}{\partial y}(\boldsymbol{F} + \boldsymbol{F_v}) + \frac{\partial}{\partial z}(\boldsymbol{G} + \boldsymbol{G_v}) = \boldsymbol{S} \tag{5}$$

where $\boldsymbol{Q}$ denotes the conservative variable vector, $\boldsymbol{E}$, $\boldsymbol{F}$, $\boldsymbol{G}$ are inviscid flux vectors, $\boldsymbol{Ev}$, $\boldsymbol{Fv}$, $\boldsymbol{Gv}$ are viscid flux vectors, $\boldsymbol{S}$ denotes the source term vector.

Turbulence model is adopted for calculation of the turbulent viscosity. Since the turbulence model is still an aspect with large uncertainty in CFD simulation. Four commonly used turbulence models (k-ε, k-ω, S-A and SST [10]) are selected for comparison of the effect on optimisation results. Second-order accuracy is obtained by Total Variation Diminishing (TVD) scheme and steady solution is achieved by implicit method. Validation of the CFD method is performed by comparison of simulation result and experimental data. The case considered has a Mach number of 0.734 at an angle of attack of 2.79 °, and the Reynolds number is about 6.3 million [11]. Adiabatic viscous wall is set for the simulation, and the free-stream turbulence intensity and temperature are 2% and 255.56K separately. Parallel computing is achieved by Message Passing Interface (MPI) to enhance the efficiency of the calculation. As shown in figure 2, good agreement is achieved between the CFD and experimental data, which demonstrates that the numerical simulation method is accurate for prediction of aerodynamic forces.

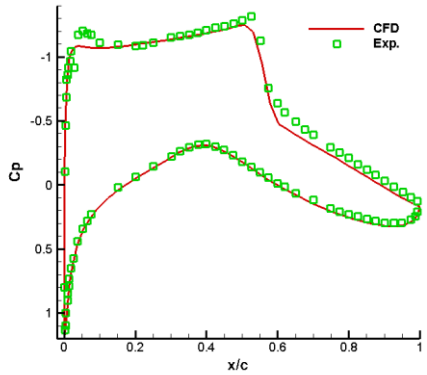

Figure 2. Pressure coefficient of the RAE2822 airfoil (SA model).

2.4. Optimization toolkit

The optimisation framework in this work is driven by the design toolkit DAKOTA, developed by Sandia National Laboratories. The toolkit has been successfully applied to several ASO problems,

such as the optimisation of a generic rocket shape[12], the helicopter rotors[13], and the hypersonic aeroshell[14]. It contains various techniques for design and optimisation, including sensitivity analysis, parameter estimation, uncertainty quantification and optimisation (gradient and non-gradient methods). Only the optimisation capability of the toolkit is utilized for the moment.

DAKOTA offers a flexible and robust interface for user's simulation codes and optimisation techniques. For simplicity and generality, connectivity between DAKOTA and optimisation modules in this work are achieved through an easy-to-use black-box interface. Flowchart of the optimisation is shown in figure 3. When an input file containing the relevant information of the problem is supplied, the automatic optimisation process starts and a parameter file with new variables is generated by DAKOTA. A FORTRAN code is then invoked to transform the parameter file to an input file requested by grid deformation. Once the CFD computation is finished, its results are extracted and transformed to the format accepted by DAKOTA, followed by new iterations until the completion of optimisation.

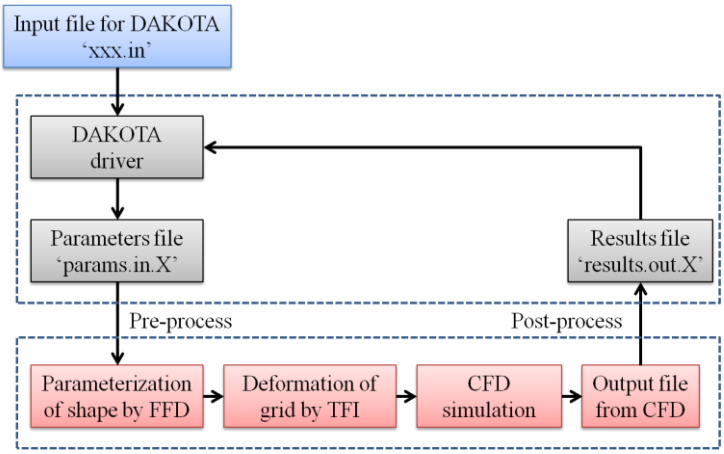

Figure 3. Flowchart of the optimization framework based on DAKOTA.

For comparison, three derivative-free global optimisation algorithms in DAKOTA are adopted, including Evolutionary Algorithms (EA), DIvision of RECTangles (DIRECT) and Efficient Global Optimisation (EGO).

The DIRECT algorithm has proven to be an effective global optimisation method for engineering applications. It is derivative free and can balance local search in promising regions with global search in unexplored regions of the design space. By subdividing the space of feasible design points, iterations can be generated in the neighbourhood of the global optimum.

The EA algorithm is a more commonly used global optimisation method based on the theory of survival of the fittest. Its key idea is that the best points in the population are allowed to survive while others are eliminated in each generation. The basic steps of EA are as follows.

1) Population initialization: a set of design points is randomly created.
2) Fitness evaluation: function evaluations are performed for each individual.
3) Parents selection: pairs of individuals are selected based on fitness value.
4) Crossover operation: apply crossover with a chosen probability for the parents.
5) Mutation operation: apply mutation with a chosen probability for the new individuals.
6) New individuals evaluation: apply function evaluations for the newly generated individuals.
7) New population determination: apply replacement to determine the new population.
8) Convergence check: return to step 2 if the loop is not converged.

Compared to DIRECT and EA, the EGO is a surrogate-based technique used for global search. In EGO, the Gaussian process (GP) model is used in each iteration for approximation of the objective function. The key idea of EGO is to maximize the Expected Improvement Function (EIF) to lead to the optimal solutions. Any new training point, which could be expected to provide better solution than

the current best solution will be selected and added to the GP model. The EGO has the following basic steps.

1) Determine a set of sample points and evaluate the objective function.
2) Construct the initial Gaussian process model.
3) Determine the new point that maximizes the EIF.
4) Evaluate the objective function at the point determined by step 3.
5) Update the Gaussian process model using the new point.
6) Return to step 3 until the loop is converged.

3. Results and discussion

3.1. Study of different optimization algorithms

Optimization cases are firstly carried out for study of effect of optimisation algorithms. The integrated framework is applied for the airfoil with the free-stream conditions from the previous validation case. For simplicity, a total of six variables are considered (shown in figure 1) and the S-A turbulence model is chosen. The original airfoil has a lift coefficient of 0.7759 and a drag coefficient of 0.01909, and the corresponding lift-drag ratio is 40.64. In all of the optimisation cases, maximization of the lift-drag ratio is adopted as the objective with the constraint that the final drag coefficient should less than its original value.

Summary of optimisation cases with different algorithms are listed in table 1. The maximum function evaluations (*Ne*) are set to 300 and 1000 for the DIRECT and EA algorithms respectively. As shown in the table, approximately 40% of increase of lift-drag ratio (denoted as *K*) has been achieved by all of the optimisation loops. Among the cases, results from the three global algorithms are very close to each other and are supposed to be the neighbours of real global optimum. The evolution-based EA algorithm has the highest objective value. However, the surrogate-based EGO algorithm is quite efficient since it requires much fewer CFD evaluations, and hence is more suitable for this kind of CPU-intensive optimisation problem.

Table 1. Summary of different cases with different optimization algorithms.

Algorithms	*Cl*	*Cd*	*K*	*Ne*
DIRECT	0.7985	0.01358	58.8	303
EA	0.8000	0.01355	59.0	1002
EGO	0.7915	0.01367	57.9	39

The iteration history of DIRECT and EA algorithms are presented in figure 4 (iteration history of the EGO algorithm is not available). It is clearly that the optimisation loops are converged since the maximal objective functions become stable after a number of iterations. Notably, the DIRECT algorithm finds its optima faster than that of the EA algorithm, and its convergence history is more oscillating because of its nature of division in the design space.

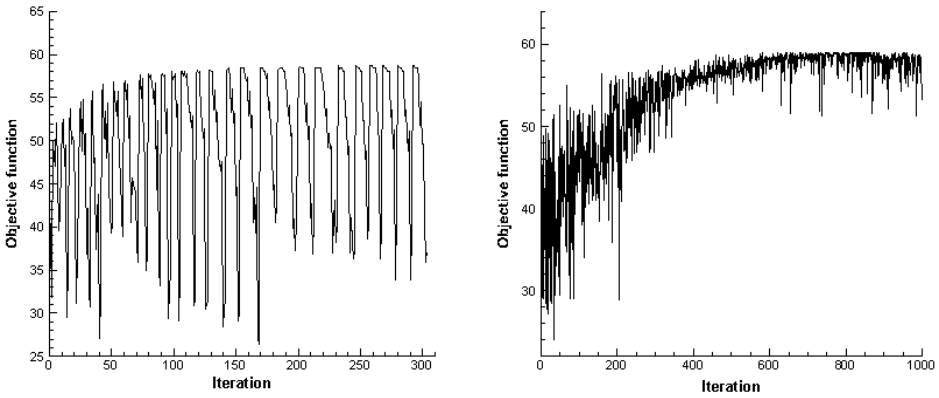

Figure 4. Convergence history of the DIRECT (left) and the EA (right) algorithm.

The comparison between the original and the optimized airfoil shapes is presented in figure 5, along with the distribution of pressure coefficient from different shapes. The optimal shapes and their pressure distribution have minor differences, especially between the results from DIRECT and EA. It can be clearly seen that the shock wave on the upper surface of optimized airfoils has been greatly eliminated. In other words, the intensive adverse pressure gradient has been significantly reduced, which results in the substantial decrease of drag force. Figure 6 shows the contours of pressure coefficient of the original and optimized (EA algorithm) airfoils. Again, the benefit of optimisation can be observed from the flow field of the shock-free airfoil.

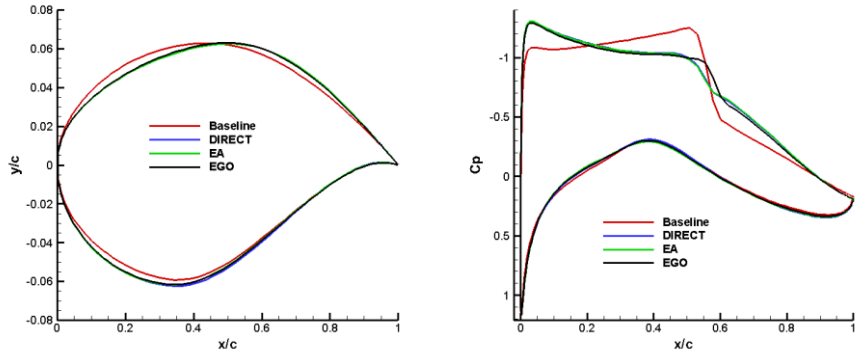

Figure 5. Airfoil shapes (left) and pressure distributions (right) .

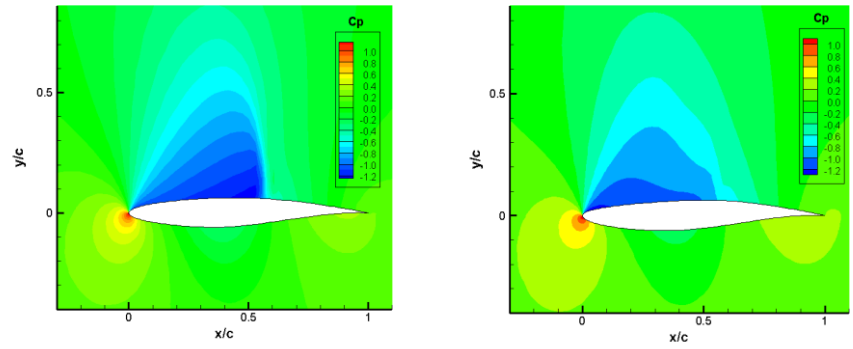

Figure 6. Pressure coefficient contour of the original (left) and optimized (right) airfoil (EA algorithm).

3.2. Study of number of design variables

Optimization cases are performed in this section for study of effect of variable number on the results. By adding control points for the control volume of FFD, numbers of design variable from 4 to 12 are compared. All optimisation loops are executed using the S-A turbulence model and efficient EGO algorithm.

Optimisations are also performed for maximization of the lift-drag ratio with the constraint of drag coefficient. Table 2 summarizes the results from different cases with different design variables. It can be observed that all of the optimized shapes have lower drag coefficient than the baseline, which means that the constraint is strictly satisfied in each of the optimisation loop. Noticeably, the objective value changes little when the optimisation has a number of design variables over 10. With the increase of design variables, the geometry shapes can be elaborately depicted, with the expansion of the design space of the optimisation problem. However, the corresponding computation resource required could be significantly increased, especially for the global optimisation using evolutionary algorithms directly. The optimal value of design variable should be a compromise of fidelity and efficiency.

Table 2. Summary of different cases with different design variables.

Number of design variables	K	Constraint (Cd-Cd_{ini})
4	55.4	-0.005747
6	57.9	-0.005426
8	60.0	-0.005079
10	61.8	-0.004740
12	61.7	-0.004898

3.3. Study of turbulence models

The final results of ASO are directly affected by the accuracy of objective function, which is obtained by CFD simulations in this work. Meanwhile, turbulence model is still one of the tough factors with large uncertainty on fluid modelling. This section explores the effect of turbulence model on the optimisation of airfoil, and all optimisation loops are executed using the efficient EGO algorithm with 10 design variables. Turbulence models considered for the same airfoil shape are the popular one equation S-A model, two-equation SST, k-ω and k-ε models.

The initial and optimized aerodynamic performance of airfoils from different turbulence models are summarized in table 3. We can see that significant improvement has been achieved by the four optimisation cases. The optimal result from SST model has the highest lift-drag ratio, while the k-ω model has the largest improvement. It is not easy to determine which model is most suitable or accurate for the case at present. However, it is clearly that the uncertainty of turbulence model has innegligible effect on the optimisation result, which has also been demonstrated in similar work [15]. Figure 7 shows the optimized airfoil shapes and the corresponding distribution of pressure coefficient from different cases. Shock reduction of different turbulence models can be clearly seen from the figure. The pressure coefficient distribution of the optimized configuration from SST model is the smoothest compared to other shapes.

Table 3. Summary of different cases with different turbulent models.

	Cl_{ini}	Cd_{ini}	K_{ini}	K_{opt}	Improvement of K
S-A	0.7759	0.01909	40.6	61.8	52.2%
SST	0.7565	0.01795	42.1	62.3	48.0%
k-ω	0.8264	0.02134	38.7	60.8	57.1%
k-ε	0.7887	0.01968	40.1	61.3	52.9%

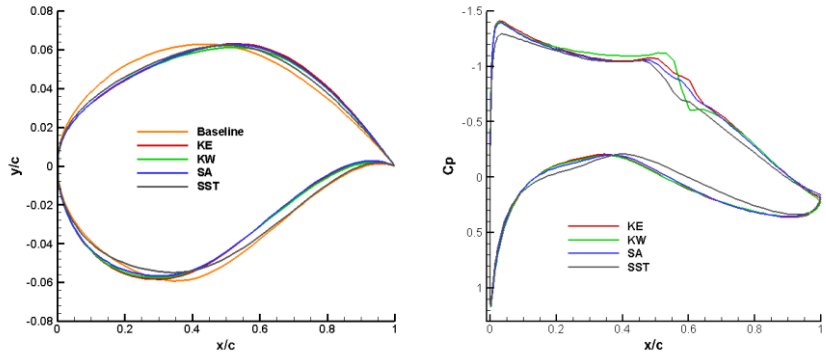

Figure 7. Optimized airfoil shapes (left) and pressure coefficients (right) from different turbulence models.

4. Conclusion

The presented work focuses on the development and demonstration of a DAKOTA-based aerodynamic shape optimisation framework. In the optimisation loop, geometry parameterization is achieved by free form deformation technique and grid deformation is carried out by a fast transfinite interpolation method. Objective functions of interest are obtained by the high-fidelity CFD simulations. Effectiveness of the framework is assessed by optimisation of the typical transonic airfoil RAE2822. Results from optimisation cases show that significant improvement of aerodynamic performance is achieved. The automatic and efficient optimisation loop can facilitate the aerodynamic design problem effectively.

For the optimisation cases considered in this work, we can see that the global method such as evolutionary algorithm is more likely to find the global optimum, while it is more time-consuming. As a compromise, the surrogate-based global method should be more appropriate for practical time-consuming engineering problems. The number of design variables and the choice of turbulence model are also important factors which should be considered carefully in the aerodynamic design process. The framework of this study could be extended to more complex aircraft configurations and even multi-disciplinary problems. Further attention will be paid to efficiency and interactivity of the optimisation loop, along with the practicability of parameterization and grid generation modules.

Acknowledgments

This research is sponsored by the Natural Science Foundation of Shanghai (Grant No. 17ZR1430100) and the State Key Development Program for Basic Research of China (Grant No. 2014CB340201).

References

[1] Chen X and Agarwal R K 2013 *Proc. Inst. Mech. Eng., Part G: J. Aerosp. Eng.* **228** 1654-67
[2] Deepak N R, Ray T and Boyce R R 2008 *J. Spacecraft Rockets* **45** 428-37
[3] Gao T, Cui K, Wang X, Hu S, Yang G and Ren L 2012 *Chin. Sci. Bull* **57** 849-57
[4] Epstein B and Peigin S 2007 *Comput. Fluids* **36** 1399-414
[5] Jahangirian A and Shahrokhi A 2011 *Comput. Fluids* **46** 270-76
[6] Lyu Z and Martins J 2013 *Proc. of the 21st AIAA Computational Fluid Dynamics Conference* San Diego
[7] Adams B M, Ebeida M S, Eldred M S, Jakeman J D, Swiler L P, Stephens J A, Vigil D M, Weldey T M, Bohnhoff W J, Dalbey K R, et al. 2016 *DAKOTA version 6.5 user's manual* SAND 2014-4633
[8] Sederberg T W and Parry S R 1986 *Proc. of the 13th Annual Conference on Computer Graphics and Interactive Techniques* New York
[9] Thompson J F, Soni B K and Weatherill N P 1998 *Handbook of Grid Generation* (CRC Press)
[10] Wilcox D C 2006 *Turbulence modeling for CFD* (DCW Industries)
[11] Cook P H, Mcdonald M A and Firmin F C P 1979 *AGARD report*, AR 138

[12] Kim J E, Rao V N, Koomullil R P, Ross D H, Soni B K and Shih A M 2009 *Math. Comput. Simul* **79** 2373-84
[13] Imiela M 2012 *Aerosp. Sci. Technol.* **23** 2-16
[14] Neville A G, Candler G V 2015 *J. of Spacecraft Rockets* **52** 76-88
[15] Guo C, Kipouros T, Shapiro E, Savvaris A 2012 *Proc. of the 53rd AIAA/ASME/ASCE/AHS/ASC Structures, Structural Dynamics and Materials Conference* Honolulu